Available online at www.sciencedirect.com
ScienceDirect
Journal of Sound and Vibration 300 (2007) 932–948
JOURNAL OF SOUND AND VIBRATION
www.elsevier.com/locate/jsvi

Tuned mass damper with nonlinear viscous damping

F. Rüdinger

Ødegaard & Danneskiold-Samsøe A/S, Titangade 15, DK-2200 Copenhagen N, Denmark

Received 30 September 2004; received in revised form 6 July 2006; accepted 12 September 2006
Available online 28 November 2006

Abstract

This paper investigates the effect of tuned mass dampers with nonlinear viscous damping elements. The tuned mass damper is assumed to be attached to a single-degree-of-freedom system excited by white noise. Statistical linearization is used to analyze the system and the accuracy of this procedure is verified by stochastic simulation. The optimal linear tuned mass damper is defined in terms of minimizing the standard deviation of the structural displacement. The structural damping is shown to have little influence on the optimal parameter values for the linear tuned mass damper. The (approximate) optimal nonlinear tuned mass damper is defined as the system, which by statistical linearization identifies an optimal equivalent linear tuned mass damper. This is shown to lead to explicit expressions for the optimal parameter values of the nonlinear tuned mass damper. The fact that statistical linearization leads to very accurate results, implies that the optimal nonlinear tuned mass damper is practically as effective as a linear tuned mass damper. However, the nonlinear tuned mass damper must be tuned to a specific amplitude and excitation intensity, in contrast to a conventional linear tuned mass damper. The theory is demonstrated for a tuned mass damper with viscous power-law damping and for a tuned mass damper with Bingham-type damping. The probability distribution of the displacement of the structure seems to be a close approximation to a Gaussian distribution despite the nonlinearity. Furthermore, it is shown by stochastic simulation, that the approximate optimal nonlinear tuned mass damper (identified via statistical linearization) is in fact very close to the true optimum.

1. Introduction

Lightly damped structures may experience large vibrations when subjected to dynamic loading. Examples include wind load on high rise buildings, towers and chimneys, wind and wave load on offshore structures and bridges and earthquake excitation of all types of structures. The vibration may lead to fatigue damage or structural collapse, and measures will therefore often be taken to reduce the vibrations, either in the design phase, or by retrofitting an existing structure.

Installation of a tuned mass damper is one way of reducing the vibration level of the structure. The tuned mass damper is an additional mass attached to the primary structure by a spring and a damper in parallel, and it was shown by Den Hartog [1], how the spring and damper coefficients should be chosen, in order to minimize the maximum frequency response of a given structural mode. This method by Den Hartog is sometimes referred to as the fixed points theory, and it was shown by Snowden [2], how it can be used for

E-mail address: fru@oedan.dk.

0022-460X/$ - see front matter © 2006 Elsevier Ltd. All rights reserved.
doi:10.1016/j.jsv.2006.09.009

systems, where the damping is introduced via a complex stiffness. In this case the excitation is assumed to be harmonic. Alternatively, one can assume a white-noise excitation, i.e. a random signal with a flat spectrum. The structural response is then minimized by minimizing the area under the frequency response function, which is proportional to the variance of the response. A number of optimal solutions for various types of excitation and various optimization objectives have been given by e.g. Warburton and Ayorinde [3–6], for several types of structural elements. Active tuned mass dampers have been considered by e.g. Ankireddi and Yang [7] minimizing the variance of the structural response, and by Ricciardelli et al. [8] using linear quadratic regulator theory.

In the papers mentioned above, the damping element connecting the additional mass is assumed to be linear. However, many commercially available dampers do display nonlinear viscous behavior. One example is the Jarret Elastomeric Spring Damper, which obeys a nonlinear viscous power law with reasonable accuracy, Terenzi [9]. Devices, where the damping is obtained by friction between structural elements, are examples of other nonlinear types of behavior experienced in engineering practice, see e.g. Ref. [10]. The optimum performance of a tuned mass damper with friction was studied by Inaudi and Kelly [11] using statistical linearization. Ricciardelli and Vickery [12] considered dry friction in a tuned mass damper with harmonic excitation.

In the present paper, the damping device connecting the primary and secondary mass is assumed to behave according to a nonlinear viscous law. The excitation is given by a white-noise process, and the objective of the passive control is to minimize the variance of the displacement of the structure. The nonlinear system is analyzed by statistical linearization and stochastic simulation taking the structural damping into account. Statistical linearization is relatively simple to use compared to methods such as stochastic averaging or perturbation techniques. If statistical linearization is sufficiently accurate to be applied for design purposes, it should therefore be unnecessary to use these more complicated approaches. Stochastic simulation is mainly used to assess the accuracy of the statistical linearization procedure for the system considered.

2. Equations of motion

A schematic model of the tuned mass damper is shown in Fig. 1. The equations of motion are given by

$$(m_1 + m_2)\ddot{x}_1 + m_2\ddot{x}_2 + c_1\dot{x}_1 + k_1 x_1 = m_1 W(t),$$
$$m_2\ddot{x}_1 + m_2\ddot{x}_2 + F_d(\dot{x}_2) + k_2 x_2 = 0 \quad (1a, b)$$

in which m_1 is the effective mass of the structure or structural component (primary mass), and m_2 is the mass of the tuned mass damper (secondary mass). m_2 will often be much smaller than m_1 for practical reasons. k_1 is the effective stiffness of the structure, and k_2 is the stiffness of the device connecting the tuned mass damper to the structure. The structure is assumed to have a small linear viscous damping with damping coefficient c_1. The displacement of the structure is denoted x_1, and the relative displacement between the structure and the tuned mass damper is denoted x_2. A dot indicates the derivative with respect to time. The damping device connecting the primary and secondary mass exerts a viscous force $F_d(\dot{x}_2)$ between the two elements. $m_1 W(t)$ is the external force, which is assumed to be a white-noise,

$$E[W(t)W(t+\Delta t)] = 2\pi S_W \delta(\Delta t), \quad (2)$$

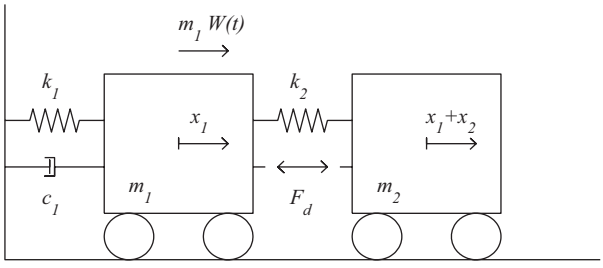

Fig. 1. Schematic model of tuned mass damper.

where scaling by m_1 is chosen for convenience. $E[\,]$ is the mean value operator, and $\delta(\,)$ is the Dirac delta function. S_W is the intensity of the white noise $W(t)$.

Initially, the primary structure is considered without the tuned mass damper. This corresponds to the case where $m_2 = 0$. The equation of motion is in this case given by

$$\ddot{x}_1 + 2\zeta_1\omega_1\dot{x}_1 + \omega_1^2 x_1 = W(t), \quad \zeta_1 = \frac{c_1}{2\sqrt{m_1 k_1}}, \quad \omega_1 = \sqrt{\frac{k_1}{m_1}}, \tag{3a–c}$$

where ζ_1 is the damping ratio, and ω_1 is the natural frequency for the structure without the tuned mass damper. The system is seen to be a simple linear oscillator excited by white noise, and the standard deviation of the response is given by, see e.g. Ref. [13], Example 3–12,

$$x_0 = \sqrt{\frac{\pi S_W}{2\zeta_1\omega_1^3}} = \sqrt{\frac{m_1^2\pi S_W}{c_1 k_1}}, \tag{4}$$

which is a measure of the magnitude of the displacement. x_0 is used as a length scale of the response. Choosing ω_1^{-1} as a time scale, the non-dimensional displacements and time are given by

$$y_i = \frac{x_i}{x_0}, \quad \tau = \omega_1 t. \tag{5a,b}$$

With this non-dimensional time the single-degree-of-freedom system has a period of 2π. Introducing these non-dimensional variables the equations of motion can be written as

$$\begin{aligned} &(1+\mu)\ddot{y}_1 + \mu\ddot{y}_2 + 2\zeta_1\dot{y}_1 + y_1 = U(\tau), \\ &\mu\ddot{y}_1 + \mu\ddot{y}_2 + f_d(\dot{y}_2) + \gamma^2\mu y_2 = 0, \end{aligned} \tag{6a, b}$$

where μ, γ and $f_d(\dot{y}_2)$ are given by

$$\mu = \frac{m_2}{m_1}, \quad \gamma = \frac{\omega_2}{\omega_1}, \quad \omega_2 = \sqrt{\frac{k_2}{m_2}}, \quad f_d(\dot{y}_2) = \frac{F_d(\dot{x}_2)}{x_0 k_1} \tag{7a–d}$$

in which μ is the mass ratio, and γ is the ratio between the frequency of the damper ω_2 and the frequency of the structure. $f_d(\dot{y}_2)$ is a non-dimensional viscous damping force. The intensity of the non-dimensional white noise $U(\tau) = W(t)/(m_1 x_0 \omega_1^2)$ can be shown to be

$$S_U = \frac{2\zeta_1}{\pi} \tag{8}$$

The non-dimensional system is seen to depend only on the parameters μ, γ, ζ_1 and the parameters describing the non-dimensional viscous damping force $f_d(\dot{y}_2)$. It is observed, that the standard deviation of the structure is unity in this formulation, when the tuned mass damper is absent.

3. Statistical linearization

Statistical linearization is now applied to replace the nonlinear equations of motion by a set of equivalent linear equations. The nonlinear (Eq. 6b) is replaced by

$$\ddot{y}_1 + \ddot{y}_2 + 2\zeta_2\gamma\dot{y}_2 + \gamma^2 y_2 = 0, \tag{9}$$

where the nonlinear damping term $f_d(\dot{y}_2)$ has been replaced by the linear damping term $2\zeta_2\gamma\mu\dot{y}_2$, and the equation has been divided by μ. ζ_2 is here an equivalent damping ratio for the secondary system, i.e. $\zeta_2 = c_{2,\mathrm{eq}}/2\sqrt{m_2 k_2}$, if the term $c_{2,\mathrm{eq}}\dot{x}_2$ is used to replace $F_d(\dot{x}_2)$ in the original Eq. (1b). The relation between the original nonlinear system and the equivalent linear system is established by minimizing the variance of the difference between the right-hand side of the two systems in the least-squares sense, see e.g. Ref. [14].

ζ_2 is obtained by

$$2\zeta_2\gamma\mu = E\left[\frac{\partial}{\partial\dot{y}_2}f_d(\dot{y}_2)\right] = \int_{-\infty}^{\infty} p_{\dot{y}_2}(\dot{y}_2)\frac{\partial}{\partial\dot{y}_2}f_d(\dot{y}_2)\,\mathrm{d}\dot{y}_2, \tag{10}$$

where $p_{\dot{y}_2}(\dot{y}_2)$ is the probability density of $\dot{y}_2$. Eq. (10) can be evaluated, if the probability density of the equivalent linear system is used in the evaluation of the integral, an approach frequently used in connection with statistical linearization. For the equivalent linear system the distribution for $\dot{y}_2$ is Gaussian

$$p_{\dot{y}_2}(\dot{y}_2) = \frac{1}{\sqrt{2\pi}\sigma_{\dot{y}_2}}\exp\left(-\frac{\dot{y}_2^2}{2\sigma_{\dot{y}_2}^2}\right), \tag{11}$$

where $\sigma_{\dot{y}_2}$ is the standard deviation of $\dot{y}_2$. $\sigma_{\dot{y}_2}$ can be evaluated from the linear system Eq. (6a), and Eq. (9) by

$$\sigma_{\dot{y}_2}^2 = S_U\int_{-\infty}^{\infty}|H_{\dot{y}_2}(r)|^2\,\mathrm{d}r, \tag{12}$$

where $H_{\dot{y}_2}(r)$ is the frequency response function relating $U(\tau)$ and $\dot{y}_2$ in the frequency domain. The frequency response function is determined by assuming harmonic excitation and harmonic response,

$$y_j = A_j\mathrm{e}^{\mathrm{i}r\tau}, \quad \dot{y}_j = \mathrm{i}rA_j\mathrm{e}^{\mathrm{i}r\tau}, \quad U(\tau) = U_0\mathrm{e}^{\mathrm{i}r\tau}, \tag{13a–c}$$

where r is a non-dimensional excitation frequency and i is the imaginary unit. The frequency response function is defined as the ratio between the response and the excitation. Substituting the expressions in Eq. (13) into the equivalent linear equations of motion, the following expression is obtained:

$$H_{\dot{y}_2}(r) = \frac{\mathrm{i}rA_2}{U_0} = \frac{\mathrm{i}r^3}{(-(1+\mu)r^2 + 2\zeta_1\mathrm{i}r + 1)(-r^2 + 2\zeta_2\gamma\mathrm{i}r + \gamma^2) - \mu r^4}. \tag{14}$$

The integral in the expression in Eq. (12) can in the present case be evaluated analytically. Using formulas from Gradshteyn and Ryzhik [15] the expression is evaluated as

$$\sigma_{\dot{y}_2}^2 = \frac{\pi S_U}{2(\lambda-\mu)}\frac{\lambda\zeta_1\gamma^3 + \zeta_2 + 4\zeta_1\zeta_2\gamma\psi}{\mu\psi^2\gamma + \zeta_1\zeta_2(1+4\zeta_1\gamma\psi) + \lambda\zeta_1\zeta_2\gamma^2(4\zeta_2\psi - 2 + \lambda\gamma^2)},$$
$$\lambda = 1+\mu, \quad \psi = \zeta_1\gamma + \zeta_2. \tag{15a–c}$$

Alternatively, $\sigma_{\dot{y}_2}$ can be obtained by solving the Lyapunov equation corresponding to the equivalent linear system Eqs. (6a) and (9). It is observed that Eq. (10) is implicit, since $\sigma_{\dot{y}_2}$ depends on ζ_2.

4. Optimal solution for equivalent linear system

The optimal solution for the equivalent linear system is defined as the solution, which minimizes the standard deviation of the response σ_{y_1}. If $\sigma_{y_1} = 1$, the tuned mass damper has no effect, and if $\sigma_{y_1} = 0$, the vibration of the primary structure is completely suppressed. The value will generally be in the range $0 < \sigma_{y_1} < 1$, when the tuned mass damper is installed. The standard deviation of the response is evaluated as

$$\sigma_{y_1}^2 = S_U\int_{-\infty}^{\infty}|H_{y_1}(r)|^2\,\mathrm{d}r, \tag{16}$$

where $H_{y_1}(r)$ is the frequency response function relating $U(\tau)$ and y_1 in the frequency domain. Substituting the expressions in Eq. (13) into (6a) and (9), this frequency response function is determined as

$$H_{y_1}(r) = \frac{A_1}{U_0} = \frac{-r^2 + 2\zeta_2\gamma\mathrm{i}r + \gamma^2}{(-(1+\mu)r^2 + 2\zeta_1\mathrm{i}r + 1)(-r^2 + 2\zeta_2\gamma\mathrm{i}r + \gamma^2) - \mu r^4}. \tag{17}$$

Again, formulas from Gradshteyn and Ryzhik [15] are used to evaluate the integral in Eq. (16). $\sigma_{y_1}^2$ is determined as

$$\sigma_{y_1}^2 = \frac{\pi S_U}{2} \frac{\zeta_2 + \psi(4\zeta_1\zeta_2\gamma + \mu\gamma^2) + \lambda\zeta_2\gamma^2(4\zeta_2\psi - 2 + \lambda\gamma^2)}{\mu\psi^2\gamma + \zeta_1\zeta_2(1 + 4\zeta_1\gamma\psi) + \lambda\zeta_1\zeta_2\gamma^2(4\zeta_2\psi - 2 + \lambda\gamma^2)}, \tag{18}$$

where λ and ψ are given in Eq. (15). The optimal values of γ and ζ_2, which minimize the variance of the response, can be determined by identifying the stationary points of $\sigma_{y_1}^2$. This corresponds to solving the two equations

$$\frac{\partial\sigma_{y_1}^2}{\partial\gamma} = 0, \quad \frac{\partial\sigma_{y_1}^2}{\partial\zeta_2} = 0. \tag{19a,b}$$

The solution to these two equations cannot to the authors knowledge be given in closed form in the general case. However, if the structural damping is neglected, the solution can be obtained. For $\zeta_1 \to 0$ Eqs. (19a,b) yield the following solution:

$$\gamma^{\text{opt}} = \sqrt{\frac{2+\mu}{2(1+\mu)^2}}, \quad \zeta_2^{\text{opt}} = \sqrt{\frac{\mu(4+3\mu)}{8(1+\mu)(2+\mu)}} \quad \text{for } \zeta_1 = 0, \tag{20a,b}$$

where γ^{opt} and ζ_2^{opt} are used to denote the optimal values of γ and ζ_2, respectively, for the equivalent linear system for $\zeta_1 \to 0$. This solution is seen to correspond to solutions given by e.g. Warburton [6] or Ankireddi and Yang [7]. For $\mu \ll 1$ Eqs. (20a,b) reduce to

$$\gamma^{\text{opt}} \simeq 1, \quad \zeta_2^{\text{opt}} \simeq \tfrac{1}{2}\sqrt{\mu} \quad \text{for } \zeta_1 = 0. \tag{21a,b}$$

The first approximation indicate, that $\omega_1 \simeq \omega_2$, i.e. that the frequency of the tuned mass damper should be approximately equal to the frequency of the structure. This is in accordance with classical results from the theory of tuned mass dampers [1]. In the case where $\zeta_1 \neq 0$, the optimal solution can be obtained numerically by determining the minimum of Eq. (18).

In Fig. 2 the results of such a procedure are shown. γ^{opt} and ζ_2^{opt} are depicted as a function of the mass ratio μ for four different values of the structural damping ratio: $\zeta_1 = 0$, 0.03, 0.1 and 0.3. The results are obtained by using the MATLAB function FMINSEARCH, and by Eqs. (20a,b) for $\zeta_1 = 0$. As seen from Fig. 2b, it is impossible to distinguish the four lines, and the influence of ζ_1 on ζ_2^{opt} is thus seen to be negligible. In Fig. 2a the lines can be distinguished, but only in the case where $\zeta_1 = 0.3$ does the line deviate significantly from the solid line representing $\zeta_1 = 0$. From the results shown in Fig. 2 it seems reasonable to assume, that ζ_1 can be neglected in the evaluation of γ^{opt} and ζ_2^{opt}, i.e. that these two parameters can be determined by Eqs. (20a,b).

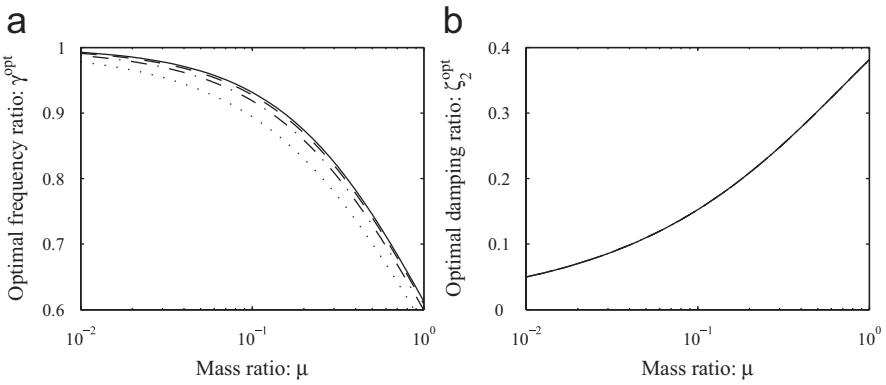

Fig. 2. (a) Optimal frequency ratio and (b) optimal damping ratio, (–) $\zeta_1 = 0$, (- -) $\zeta_1 = 0.03$, (- · -) $\zeta_1 = 0.1$, (· · ·) $\zeta_1 = 0.3$.

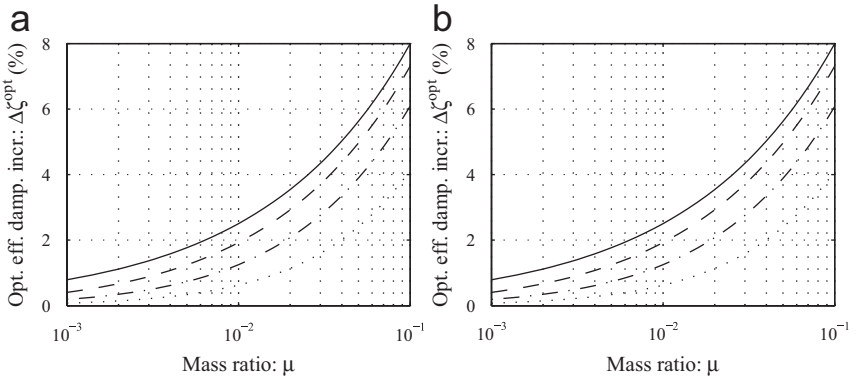

Fig. 3. Optimal effective damping increase: (a) exact and (b) approximation, (–) $\zeta_1 = 0$, (- -) $\zeta_1 = 0.03$, (- · -) $\zeta_1 = 0.1$, (···) $\zeta_1 = 0.3$.

In order to investigate this point further, the effective damping of the system is considered. By analogy with a single-degree-of-freedom system the effective damping ratio is introduced as, see Ref. [16],

$$\zeta_e = \frac{\pi S_W}{2\omega_1^3 \sigma_{x_1}^2} = \frac{\zeta_1}{\sigma_{y_1}^2}. \tag{22}$$

The effective damping increase is then defined as

$$\Delta\zeta = \zeta_e - \zeta_1. \tag{23}$$

The effective damping increase can be evaluated analytically from Eq. (18) as

$$\Delta\zeta = \frac{\mu\zeta_2\psi\gamma}{\zeta_2 + \psi(4\zeta_1\zeta_2\gamma + \mu\gamma^2) + \lambda\zeta_2\gamma^2(4\zeta_2\psi - 2 + \lambda\gamma^2)} \tag{24}$$

with λ and ψ defined in Eq. (15). The optimal effective damping increase $\Delta\zeta^{opt}$ is obtained by evaluating $\Delta\zeta$ for γ^{opt} and ζ_2^{opt}. For $\zeta_1 = 0$ the optimal value is given by inserting Eqs. (20a,b) in the expression for $\Delta\zeta$ for $\zeta_1 = 0$. $\Delta\zeta^{opt}$ is then given by

$$\Delta\zeta^{opt} = \sqrt{\frac{(1+\mu)\mu}{16 + 12\mu}} \quad \text{for } \zeta_1 = 0. \tag{25}$$

For $\mu \ll 1$, $\Delta\zeta^{opt}$ is approximated by

$$\Delta\zeta^{opt} \simeq \tfrac{1}{4}\sqrt{\mu} \simeq \tfrac{1}{2}\zeta_2^{opt} \quad \text{for } \zeta_1 = 0. \tag{26}$$

The tuned mass damper is thus seen to increase the effective damping ratio of the system by approximately half the value of the damping ratio of the tuned mass damper. For $\zeta_1 \neq 0$, γ^{opt} and ζ_2^{opt} are not known analytically. However, an approximation to $\Delta\zeta^{opt}$ can be obtained by assuming, that γ^{opt} and ζ_2^{opt} can be approximated by Eqs. (20a,b) and substituting these values into Eq. (24). This leads to the following:

$$\Delta\zeta^{opt} \simeq \frac{L_0 + L_1\zeta_1}{K_0 + K_1\zeta_1 + K_2\zeta_1^2}, \quad L_0 = \frac{\mu^2(4+3\mu)}{8(2+\mu)}, \quad L_1 = \frac{\mu^{3/2}}{4}\sqrt{\frac{4+3\mu}{1+\mu}},$$
$$K_0 = \frac{(\mu(4+3\mu))^{3/2}}{4\sqrt{1+\mu}(2+\mu)}, \quad K_1 = \frac{\mu(24+32\mu+11\mu^2)}{4(2+\mu)(1+\mu)}, \quad K_2 = \sqrt{\frac{\mu(4+3\mu)}{1+\mu}}. \tag{27a–f}$$

The expression is seen to reduce to Eq. (25) for $\zeta_1 \to 0$.

In Fig. 3 $\Delta\zeta^{opt}$ is evaluated for four different values of the structural damping: $\zeta_1 = 0$, 0.03, 0.1 and 0.3. In Fig. 3a the exact values of $\Delta\zeta^{opt}$ are evaluated by determining γ^{opt} and ζ_2^{opt} using the MATLAB function FMINSEARCH corresponding to the approach used in Fig. 2 for $\zeta_1 \neq 0$. In Fig. 3b $\Delta\zeta^{opt}$ is determined by Eq. (27),

which is only an approximation in the cases $\zeta_1 \neq 0$. Comparing the results in Fig. 3a with the results in Fig. 3b it is seen, that Eq. (27) gives a very good approximation to the optimal effective damping increase. It is furthermore seen, that $\Delta\zeta^{\text{opt}}$ increases with decreasing values of structural damping ζ_1. As indicated by Eq. (26), $\Delta\zeta^{\text{opt}}$ also increases with increasing values of μ, as one would expect. Based on the results presented in this section it is concluded, that γ^{opt} and ζ_2^{opt} can be accurately estimated from Eqs. (20a,b) for $\zeta_1 \lesssim 0.3$. In the following this approximation will be used.

5. Stochastic simulation

Stochastic simulation, also known as Monte Carlo simulation, offers an alternative to statistical linearization, when nonlinear stochastic systems are considered. Using this method a record of the excitation process is generated, and a sample of the stochastic response is obtained by direct numerical simulation of the equations of motion. This method is generally time consuming, since long records are needed to evaluate the statistics of the response. However, the method is convenient, when the quality of an approximate solution technique such as statistical linearization needs to be assessed.

The first issue to consider in connection with stochastic simulation is the simulation of the excitation record. An ideal white noise is a process with an infinite variance and a correlation time, which is infinitely small. It thus represents an idealization, which can never occur in the physical reality, and which cannot be represented by a digital record generated by a computer. The white noise applied as excitation process is thus an approximation to an ideal white noise. Consider a sequence of independent random numbers U_i, each of which has a Gaussian distribution with zero mean and standard deviation σ_U. A stochastic process $U(\tau)$ is generated by linear interpolation of the random numbers U_i, each separated by a time increment $\Delta\tau = \tau_{i+1} - \tau_i$, see Fig. 4. As can be derived from results given by Clough and Penzien [17], the power spectral density of this process is given by

$$S_U(r) = S_0 \left[\frac{\sin(\frac{1}{2} r \Delta\tau)}{\frac{1}{2} r \Delta\tau} \right]^4, \quad S_0 = \sigma_U^2 \frac{\Delta\tau}{2\pi}, \tag{28a,b}$$

where r is a non-dimensional excitation frequency. The function is shown in Fig. 4b, and it is observed, that the spectrum is approximately constant $S_U(r) \simeq S_0$ for $r\Delta\tau \ll 1$. If the system has a typical frequency $\langle r \rangle$, such that $\langle r \rangle \Delta\tau \ll 1$, the excitation will be experienced as a close approximation to white noise by the system. Due to the normalization discussed in Section 2 a typical frequency for the system is unity, i.e. $\langle r \rangle \simeq 1$. $\langle r \rangle \Delta\tau \simeq \Delta\tau$ will therefore be chosen as a small number in the following examples.

In order to carry out the numerical integration the nonlinear Eqs. (6a,b) of motion are rewritten in state-space format as

$$\dot{\mathbf{z}} = \mathbf{G}(\mathbf{z}) + \mathbf{B}U(\tau), \quad \mathbf{z}^{\mathrm{T}} = [y_1\, y_2\, \dot{y}_1\, \dot{y}_2], \tag{29a,b}$$

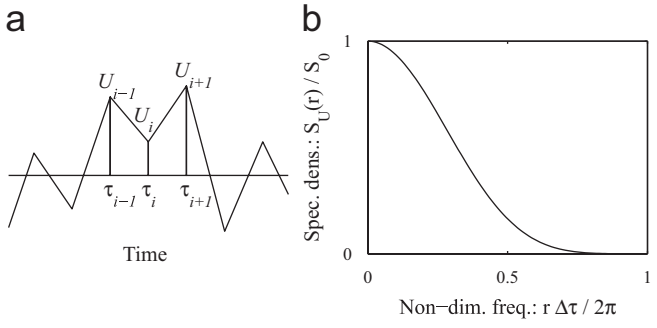

Fig. 4. (a) Piecewise linear process $U(\tau)$ and (b) spectral density of piecewise linear process.

Table 1
Algorithm for fourth-order Runge–Kutta integration

$\mathbf{z}_1 = \mathbf{G}(\mathbf{z}_i)\Delta\tau + \mathbf{B}U(\tau_i)\Delta\tau$
$\mathbf{z}_2 = \mathbf{G}(\mathbf{z}_i + \frac{1}{2}\mathbf{z}_1)\Delta\tau + \mathbf{B}(\frac{1}{2}U(\tau_i) + \frac{1}{2}U(\tau_{i+1}))\Delta\tau$
$\mathbf{z}_3 = \mathbf{G}(\mathbf{z}_i + \frac{1}{2}\mathbf{z}_2)\Delta\tau + \mathbf{B}(\frac{1}{2}U(\tau_i) + \frac{1}{2}U(\tau_{i+1}))\Delta\tau$
$\mathbf{z}_4 = \mathbf{G}(\mathbf{z}_i + \mathbf{z}_3)\Delta\tau + \mathbf{B}U(\tau_{i+1})\Delta\tau$
$\mathbf{z}_{i+1} = \mathbf{z}_i + \frac{1}{6}\mathbf{z}_1 + \frac{1}{3}\mathbf{z}_2 + \frac{1}{3}\mathbf{z}_3 + \frac{1}{6}\mathbf{z}_4$

where $\mathbf{z}$ is a non-dimensional state-space vector, and $U(\tau)$ is the excitation process generated by the procedure described in the previous paragraph. $\mathbf{G}(\mathbf{z})$ and $\mathbf{B}$ are given by

$$\mathbf{G}(\mathbf{z}) = \begin{bmatrix} 0 & 0 & 1 & 0 \\ 0 & 0 & 0 & 1 \\ \dfrac{-1}{\lambda-\mu} & \dfrac{\gamma^2\mu}{\lambda-\mu} & \dfrac{-2\zeta_1}{\lambda-\mu} & 0 \\ \dfrac{1}{\lambda-\mu} & \dfrac{-\lambda\gamma^2}{\lambda-\mu} & \dfrac{2\zeta_1}{\lambda-\mu} & 0 \end{bmatrix} \mathbf{z} - \begin{bmatrix} 0 \\ 0 \\ \dfrac{-f_d(z_4)}{\lambda-\mu} \\ \dfrac{\lambda f_d(z_4)}{\lambda\mu-\mu^2} \end{bmatrix},$$

$$\mathbf{B}^{\mathrm{T}} = \begin{bmatrix} 0 & 0 & \dfrac{1}{\lambda-\mu} & \dfrac{-1}{\lambda-\mu} \end{bmatrix} \tag{30a, b}$$

with λ given by Eq. (15b). The integration procedure, which is used, is fourth-order Runge–Kutta integration. The algorithm of this integration scheme is given in Table 1, where it is assumed, that the state-space vector $\mathbf{z}_i$ at time τ_i is known, and the state-space vector $\mathbf{z}_{i+1}$ at time τ_{i+1} is evaluated.

6. Examples of systems with nonlinear viscous damping

In order to investigate the accuracy of the statistical linearization procedure for tuned mass dampers with nonlinear damping, two examples are considered in the following. It is assumed that optimal tuning is used for the mass damper, so the theoretical results obtained by statistical linearization are only investigated in the vicinity of this optimum.

6.1. Viscous power-law damping

The first example is a damping force, which obeys a nonlinear viscous power law. This force is expressed as

$$F_d(\dot{x}_2) = \beta \,\mathrm{sign}\,(\dot{x}_2)\,|\dot{x}_2|^{\nu}, \tag{31}$$

where β is the damping coefficient and has the dimension mass $\times$ length$^{1-\nu}$ $\times$ time$^{\nu-2}$, and ν is termed the power-law exponent. It is assumed that ν is given for a specific type of dampers, and that the objective is to determine the optimal size of the damper by selecting the right coefficient β. A damping of this type has been shown to give a reasonable representation of the behavior of the Jarret Elastomeric Spring Damper, Terenzi [9]. Lin and Chopra [18] have considered this type of damping in the investigation of earthquake-induced response. The probabilistic characteristics of an oscillator with this type of damping and white-noise excitation was studied by Rüdinger and Krenk [19]. For $\nu = 1$ the linear viscous damping law is retrieved, and for $\nu = 0$ the case of dry friction appears. Rescaling by Eq. (7d) yields

$$f_d(\dot{y}_2) = \eta \,\mathrm{sign}(\dot{y}_2)\,|\dot{y}_2|^{\nu}, \quad \eta = \beta\frac{m_1^{(\nu-2)/2}}{\sqrt{k_1}}\left(\frac{\pi S_W}{c_1}\right)^{(\nu-1)/2}, \tag{32a,b}$$

where η is a non-dimensional damping coefficient. η will normally be assumed to be the design parameter, while v will be fixed for the specific type of damper. The derivative of Eq. (32) is given by

$$\frac{\partial f_d(\dot{y}_2)}{\partial \dot{y}_2} = \eta v\,|\dot{y}_2|^{v-1}. \tag{33}$$

The expression in Eq. (10) relating the nonlinear system to the equivalent linear system can now be evaluated as

$$2\zeta_2\gamma\mu = \int_{-\infty}^{\infty} \frac{\eta v\,|\dot{y}_2|^{v-1}}{\sqrt{2\pi}\sigma_{\dot{y}_2}} \exp\left(-\frac{\dot{y}_2^2}{2\sigma_{\dot{y}_2}^2}\right) \mathrm{d}\dot{y}_2 = \frac{\eta v\,\Gamma(\frac{1}{2}v)\,(\sqrt{2}\sigma_{\dot{y}_2})^{v-1}}{\sqrt{\pi}}. \tag{34}$$

If v is assumed given, the optimal value of the nonlinear damping coefficient η^{opt} is obtained by inserting the optimal values of ζ_2 and γ in Eq. (34). η^{opt} is then given by

$$\eta^{\mathrm{opt}} = \frac{\sqrt{\pi}(\sqrt{2}\sigma_{\dot{y}_2})^{1-v}}{v\,\Gamma(\frac{1}{2}v)} 2\mu\zeta_2^{\mathrm{opt}}\gamma^{\mathrm{opt}}, \tag{35}$$

where ζ_2^{opt} and γ^{opt} can be approximated by Eqs. (20a,b) for small levels of structural damping. The standard deviation of the non-dimensional relative velocity $\sigma_{\dot{y}_2}$ is evaluated by Eq. (15) using optimal values for ζ_2 and γ. It is observed, that Eq. (35) is explicit, since $\sigma_{\dot{y}_2}$ does not depend on η.

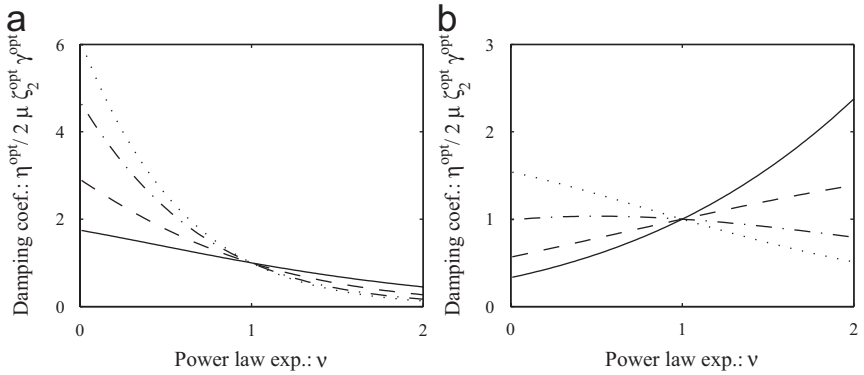

Fig. 5. Optimal nonlinear damping coefficient as function of power-law exponent, (–) $\zeta_1 = 0.001$, (- -) $\zeta_1 = 0.003$, (- · -) $\zeta_1 = 0.01$, (···) $\zeta_1 = 0.03$, (a) $\mu = 0.01$ and (b) $\mu = 0.1$.

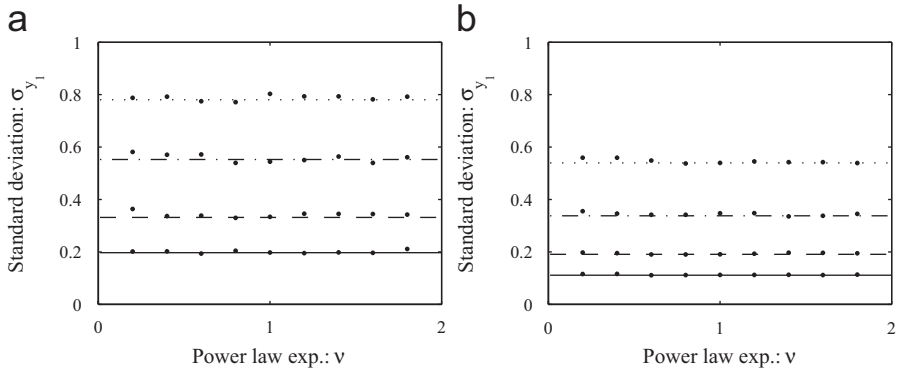

Fig. 6. Standard deviation as function of power-law exponent for optimal parameters, (–) $\zeta_1 = 0.001$, (- -) $\zeta_1 = 0.003$, (- · -) $\zeta_1 = 0.01$, (···) $\zeta_1 = 0.03$, (•) simulation, (a) $\mu = 0.01$ and (b) $\mu = 0.1$.

In Fig. 5, the optimal nonlinear damping coefficient is shown as function of the power-law exponent. In Fig. 5a the mass ratio is $\mu = 0.01$, and in Fig. 5b the mass ratio is $\mu = 0.1$. In both cases four values of the structural damping ratio have been considered: $\zeta_1 = 0.001$, 0.003, 0.01 and 0.03. For $v = 1$ the results for the linear system are retrieved, i.e. $\eta^{\text{opt}} = 2\mu\zeta_2^{\text{opt}}\gamma^{\text{opt}}$. It is observed, that the structural damping ratio has a large influence on the optimal nonlinear damping coefficient, when $v \cong 1$.

In Fig. 6 the standard deviation of the non-dimensional structural displacement y_1 is evaluated as function of the power-law exponent for optimal parameter values. In Fig. 6a the mass ratio is $\mu = 0.01$, and in Fig. 6b the mass ratio is $\mu = 0.1$. Again, four values of the structural damping ratio have been considered: $\zeta_1 = 0.001$, 0.003, 0.01 and 0.03. The solid lines correspond to the theoretical results obtained by statistical linearization. The dots correspond to results obtained by stochastic simulation of the nonlinear system using a non-dimensional time step of $\Delta\tau = 2\pi/50$ (50 steps per typical period) and simulating 2000 typical periods of vibration (simulation time: $2\pi \cdot 2000$). The lines are horizontal, since for any value of v an equivalent linear system ($v = 1$) is identified, and the two systems are assumed to have the same optimal value of σ_{y_1}. The results obtained by stochastic simulation (the dots) will not be completely horizontal, since statistical linearization is only an approximation. The results from theory and simulation are seen to agree very well confirming the applicability of the statistical linearization procedure for the system investigated.

The results in Fig. 6 suggest, that the optimal parameters for the nonlinear system obtained by this procedure have the same effect as an optimal linear tuned mass damper. However, since the statistical linearization procedure is an approximation, the solution is not optimal in a strict mathematical sense, and it could be argued, that a different choice of parameter values for the nonlinear system might lead to improved performance. In Fig. 7 contour plots of σ_{y_1} are shown as functions of ζ_2 and γ for $\mu = 0.01$ and $\zeta_1 = 0.001$. In Fig. 7a $v = 0.4$, and in Fig. 7b $v = 1.4$. The contour plots are based on estimates of σ_{y_1} for 5×5 values of η and γ around the approximate optima η^{opt} and γ^{opt}. The lines in the plot show values of $\sigma_{y_1} = 0.0103, 0.0206, 0.0309, 0.0412, \ldots$. Since the plots are based on results obtained by stochastic simulation the contours are a bit irregular. All estimates of σ_{y_1} are obtained by stochastic simulation of 2000 mean periods with 50 steps per period. As seen by the figures, the optimum for the nonlinear system seems to be very close to $\eta = \eta^{\text{opt}}$ and $\gamma = \gamma^{\text{opt}}$, confirming the accuracy of using this statistical linearization procedure to determine optimal parameter values for the nonlinear tuned mass damper. It is observed from Fig. 7, that the system is much more sensitive to variations in the value of γ, than to variations in the value of η.

The next issue, which will be investigated, is the probability density of the response. Initially, the non-dimensional velocity difference $\dot{y}_2 = z_4$ is investigated. In Figs. 8 and 9, the probability density is shown for optimal damping parameters and different combinations of the mass ratio and power-law exponent. In Fig. 8 the power-law exponent is $v = 0.2$, and in Fig. 9 the power-law exponent is $v = 2$. In Figs. 8a and 9a the mass ratio is $\mu = 0.01$, and in Figs. 8b and 9b the mass ratio is $\mu = 0.1$. In all cases two different values of the structural damping ratio are considered: $\zeta_1 = 0.003$ and 0.01. The solid line corresponds to the Gaussian distribution in Eq. (11), which is the distribution of the velocity difference for the equivalent linear system. The crosses and circles represent scaled histograms of response records obtained by stochastic simulation of the

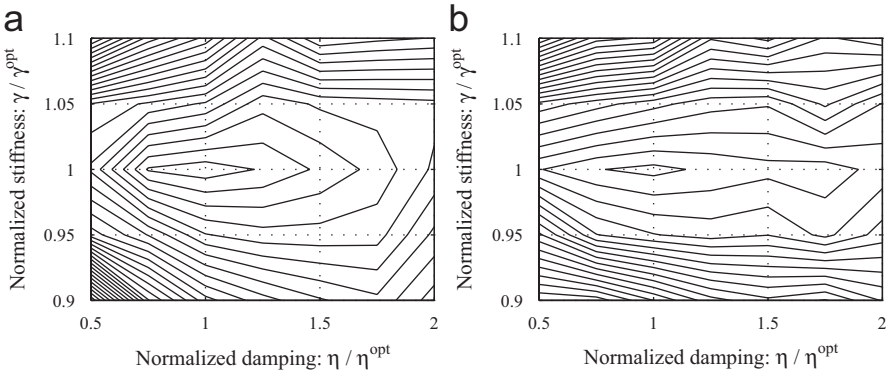

Fig. 7. Contour plots for σ_{y_1} as function of γ and η, $\mu = 0.01$, $\zeta_1 = 0.001$, (a) $v = 0.4$ and (b) $v = 1.4$.

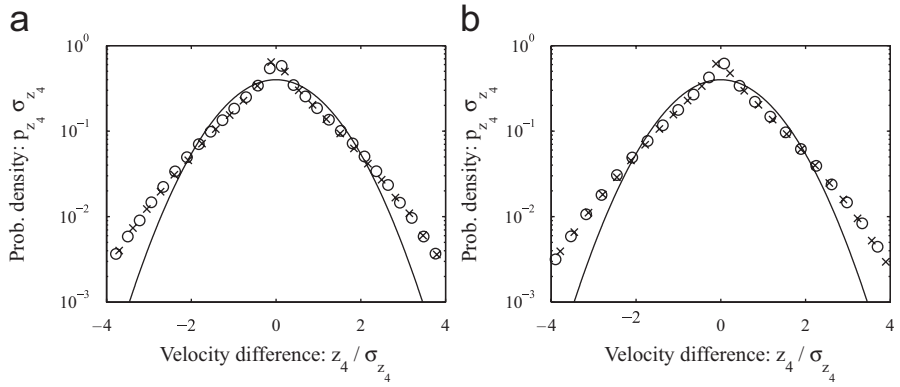

Fig. 8. Probability density of velocity difference for optimal parameters, $v = 0.2$, (a) $\mu = 0.01$ and (b) $\mu = 0.1$, (–) theoretical expression, (×) $\zeta_1 = 0.003$, (○) $\zeta_1 = 0.01$.

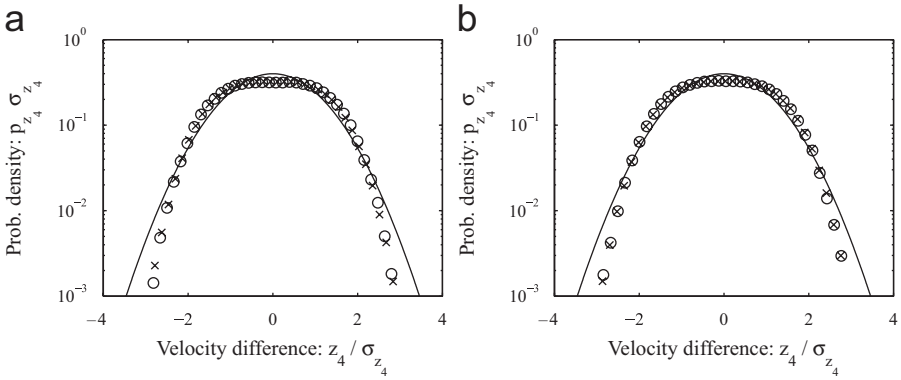

Fig. 9. Probability density of velocity difference for optimal parameters, $v = 2$, (a) $\mu = 0.01$ and (b) $\mu = 0.1$, (–) theoretical expression, (×) $\zeta_1 = 0.003$, (○) $\zeta_1 = 0.01$.

nonlinear system. The time step is the same as the one used in the simulations discussed in the previous paragraph, but in this case 20,000 typical periods have been simulated in order to obtain a good estimate of the probability density. The probability density of the nonlinear system is seen to deviate substantially from the Gaussian distribution. For $v = 0.2$ the probability density seems to approximately follow an exponential function in the range considered. For $v = 2$ the probability density has a relatively flat top and drops to zero faster than the Gaussian probability density, in contrast to the case where $v = 0.2$. In view of this deviation from the Gaussian distribution, it might seem surprising, that the statistical linearization produces such accurate results for the standard deviation of the structural displacements, as shown in Fig. 6. The structural damping is seen to have a very small effect on the probability density.

In Figs. 10 and 11 the probability density for the structural displacement is shown for the same system parameters and simulation parameters as in Figs. 8 and 9. It is observed, that the probability density for the structure with a nonlinear viscous damper is approximately Gaussian in all cases. This information would facilitate the evaluation of extreme value statistics for the nonlinear system.

6.2. Bingham model

The second example, which will be considered, is a tuned mass damper with a damping element consisting of a connection in parallel between a linear viscous damper and a dry friction element. This damping model is

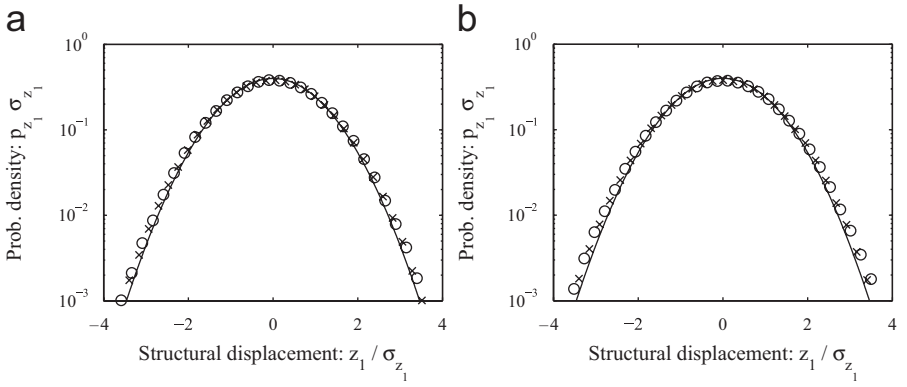

Fig. 10. Probability density of structural displacement for optimal parameters, $\nu = 0.2$, (a) $\mu = 0.01$ and (b) $\mu = 0.1$, (–) theoretical expression, (×) $\zeta_1 = 0.003$, (○) $\zeta_1 = 0.01$.

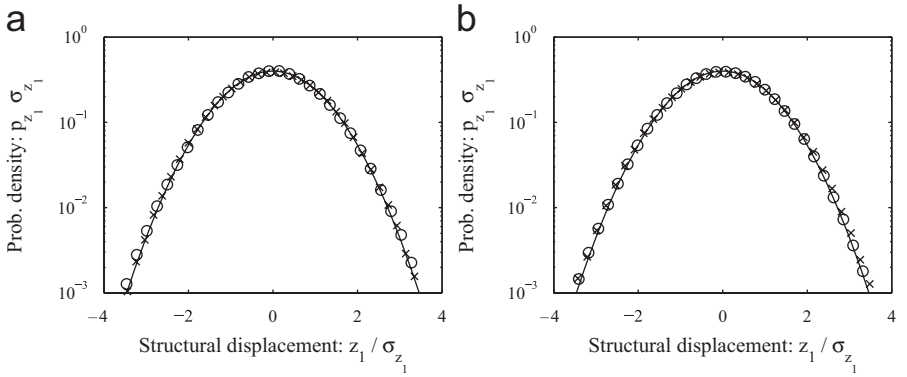

Fig. 11. Probability density of structural displacement for optimal parameters, $\nu = 2$, (a) $\mu = 0.01$ and (b) $\mu = 0.1$, (–) theoretical expression, (×) $\zeta_1 = 0.003$, (○) $\zeta_1 = 0.01$.

sometimes referred to as the Bingham model. Mathematically, this nonlinear viscous damping force can be expressed as

$$F_d(\dot{x}_2) = \beta_1 \operatorname{sign}(\dot{x}_2) + \beta_2 \dot{x}_2, \tag{36}$$

where β_1 is the dry friction damping coefficient, and β_2 is the linear viscous damping coefficient. Again, Eq. (7d) is used for rescaling, which leads to the following non-dimensional damping force:

$$f_d(\dot{y}_2) = \eta_1 \operatorname{sign}(\dot{y}_2) + \eta_2 \dot{y}_2, \quad \eta_1 = \frac{\beta_1}{m_1}\sqrt{\frac{c_1}{k_1 \pi S_W}}, \quad \eta_2 = \frac{\beta_2}{\sqrt{k_1 m_1}}, \tag{37a–c}$$

where η_1 and η_2 are non-dimensional damping coefficients related to dry friction and linear viscous damping, respectively. The derivative of this non-dimensional force is evaluated as

$$\frac{\partial f_d(\dot{y}_2)}{\partial \dot{y}_2} = 2\eta_1 \delta(\dot{y}_2) + \eta_2, \tag{38}$$

where $\delta(\,)$ is the Dirac delta function. The relationship between the nonlinear system and the equivalent linear system is established by evaluating the integral in Eq. (10)

$$2\zeta_2 \gamma \mu = \sqrt{\frac{2}{\pi \sigma_{\dot{y}_2}^2}}\,\eta_1 + \eta_2 \tag{39}$$

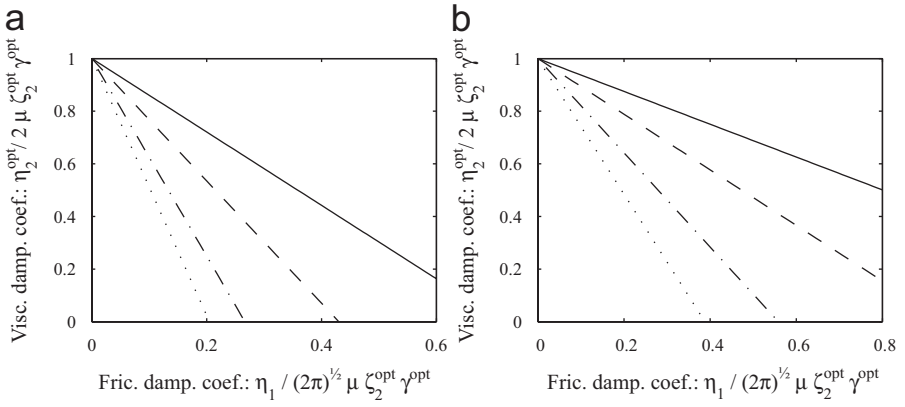

Fig. 12. Optimal viscous damping coefficient as function of friction damping coefficient, (–) $\zeta_1 = 0.001$, (- -) $\zeta_1 = 0.003$, (- · -) $\zeta_1 = 0.01$, $(\cdots)$ $\zeta_1 = 0.03$, (a) $\mu = 0.01$ and (b) $\mu = 0.1$.

The optimal nonlinear system is defined as the system, which by statistical linearization, leads to an optimal equivalent linear system. If η_2 is assumed to be given, the optimal value of η_1 is obtained as

$$\eta_1^{opt} = \sqrt{\frac{\pi\sigma_{\dot{y}_2}^2}{2}}(2\mu\zeta_2^{opt}\gamma^{opt} - \eta_2) \tag{40}$$

requiring that $\eta_2 \leqslant 2\mu\zeta_2^{opt}\gamma^{opt}$. Alternatively, if η_1 is assumed to be given, the optimal value of η_2 is obtained as

$$\eta_2^{opt} = 2\mu\zeta_2^{opt}\gamma^{opt} - \sqrt{\frac{2}{\pi\sigma_{\dot{y}_2}^2}}\eta_1. \tag{41}$$

In both cases the expressions are seen to be explicit, since $\sigma_{\dot{y}_2}$ does not depend on neither η_1 nor η_2. For given values of the mass ratio and structural damping, the optimal values of η_1 and η_2 are related linearly.

It is now assumed that the dry friction coefficient is given, and that the optimal viscous damping coefficient needs to be evaluated. In Fig. 12, the optimal viscous damping coefficient is shown as a function of the dry friction coefficient. In Fig. 12a, the mass ratio is $\mu = 0.01$ and in Fig. 12b the mass ratio is $\mu = 0.03$. Again, four values of the structural damping have been considered: $\zeta_1 = 0.001$, 0.003, 0.01 and 0.03. The linearity observed in Eq. (41) is confirmed. For large values of the dry friction coefficient the optimal linear viscous damping coefficient becomes negative. In this case the system is not realizable by a passive device. The structural damping ratio is seen to have a large influence on the optimal value of the linear viscous damping coefficient.

In Fig. 13, the standard deviation of the structural displacement y_2 is evaluated as a function of the dry friction coefficient for optimal values of the linear viscous damping coefficient. The range of parameters considered is the same as in Fig. 12, so in the upper right corner of the figure the linear viscous damping coefficient is negative. The solid lines correspond to the results obtained by statistical linearization, and the dots correspond to results obtained by stochastic simulation. The simulation parameters are the same as the ones used in the previous subsection for Fig. 6. Again, the agreement confirms the applicability of the statistical linearization procedure. This means that the vibration reduction obtained by a linear tuned mass damper for a given mass ratio can also be achieved by a tuned mass damper with nonlinear viscous damping. However, in the nonlinear case the tuning depends on the structural damping and on the excitation intensity in contrast to the linear case.

The next issue, which is considered, is the probability density of the velocity difference $\dot{y}_2 = z_4$. This probability is shown in Fig. 14 for various optimal parameter combinations. The mass ratio is $\mu = 0.03$ and the values of the nonlinear dry friction coefficient are $\eta_1/(\sqrt{2\pi}\mu\zeta_2^{opt}\gamma^{opt}) = 0.3$ and 0.5. As can be observed from Fig. 12 this leads to positive optimal values of the linear viscous damping coefficient in all cases. Two values of the structural damping ratio are considered: $\zeta_1 = 0.003$ and 0.01. The solid line corresponds to

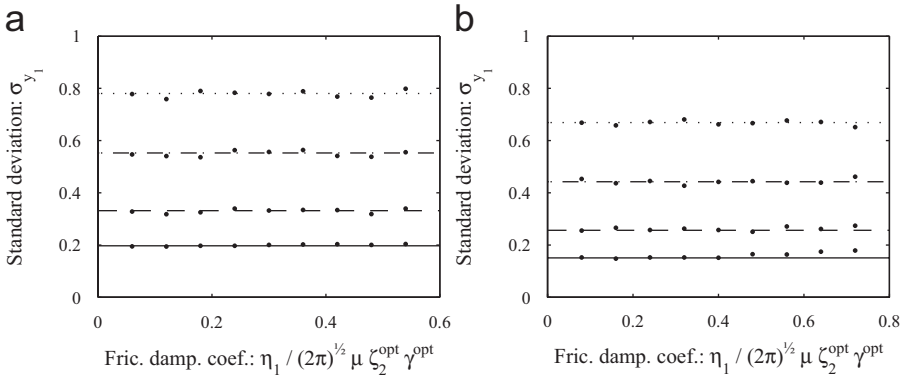

Fig. 13. Standard deviation as function of friction damping coefficient for optimal parameters, (–) $\zeta_1 = 0.001$, (- -) $\zeta_1 = 0.003$, (- · -) $\zeta_1 = 0.01$, (···) $\zeta_1 = 0.03$, (•) simulation, (a) $\mu = 0.01$ and (b) $\mu = 0.03$.

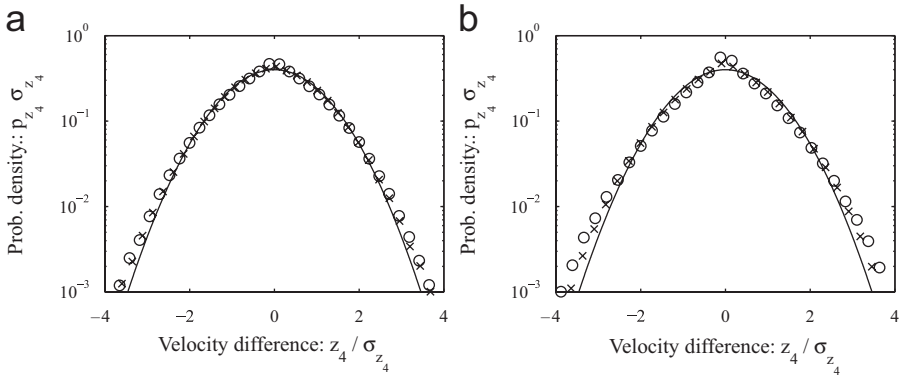

Fig. 14. Probability density of velocity difference for optimal parameters for $\mu = 0.03$, (a) $\eta_1/(\sqrt{2\pi}\mu\zeta_2^{\text{opt}}\gamma^{\text{opt}}) = 0.3$ and (b) $\eta_1/(\sqrt{2\pi}\mu\zeta_2^{\text{opt}}\gamma^{\text{opt}}) = 0.5$, (–) theoretical expression, (×) $\zeta_1 = 0.003$, (○) $\zeta_1 = 0.01$.

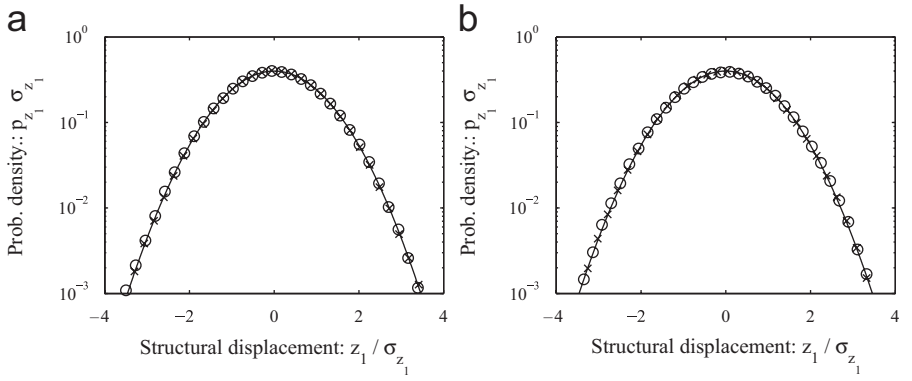

Fig. 15. Probability density of structural displacement for optimal parameters for $\mu = 0.03$, (a) $\eta_1/(\sqrt{2\pi}\mu\zeta_2^{\text{opt}}\gamma^{\text{opt}}) = 0.3$ and (b) $\eta_1/(\sqrt{2\pi}\mu\zeta_2^{\text{opt}}\gamma^{\text{opt}}) = 0.5$, (–) theoretical expression, (×) $\zeta_1 = 0.003$, (○) $\zeta_1 = 0.01$.

statistical linearization results, which lead to a Gaussian distribution, while the circles and crosses are results obtained by stochastic simulation of the nonlinear system. The simulation parameters are identical to those used for Figs. 8–11 in the previous subsection. The figures show, that the probability densities are substantially less non-Gaussian than for the case of viscous power-law damping investigated in the previous subsection. A simple explanation for this could be, that the systems considered have a smaller degree of nonlinearity.

In Fig. 15, the probability density of the structural displacement $y_1 = z_1$ is shown for the same parameters as in Fig. 14. The solid line is the Gaussian distribution resulting from the equivalent linear system obtained by statistical linearization, while the crosses and dots originate from stochastic simulation of the nonlinear system. As seen from the figure, the distribution is a very close approximation to a Gaussian distribution, as observed in the previous subsection for a tuned mass damper with power-law viscous damping.

7. Conclusion

A tuned mass damper with a nonlinear viscous damping element has been considered. The effect of this device in terms of reducing the standard deviation of the displacement of a single-degree-of-freedom system under white-noise excitation has been investigated taking the structural damping into account. Statistical linearization is used to analyze the nonlinear tuned mass damper, and the accuracy of this procedure is assessed by stochastic simulation. An approximate optimal solution for the nonlinear tuned mass damper is defined as a system, which by statistical linearization identifies an optimal linear tuned mass damper. Nonlinear tuned mass dampers with viscous power-law damping and with Bingham-type damping are used to demonstrate the procedure. An example of the design procedure for a system with viscous power-law damping is given in the appendix.

The main findings are summarized below:

- The structural damping has very little influence on the optimal parameter values for a linear tuned mass damper.
- Statistical linearization gives very accurate estimates of the standard deviation of the structural displacement. The probability distribution of the structural displacement is approximately Gaussian, while the distribution of the velocity difference between the structure and the tuned mass damper deviates substantially from a Gaussian distribution.
- The accuracy of the statistical linearization procedure implies that optimal linear and nonlinear tuned mass dampers have practically the same effect in terms of reducing the structural displacement. The approximate optimal parameter values for the nonlinear tuned mass damper obtained by this procedure are very close to the true optimal parameter values.
- The approximate optimal solution for the nonlinear tuned mass damper can be given in explicit form.
- The optimal damping parameter values for the nonlinear tuned mass damper depend on the displacement magnitude and excitation intensity, in contrast to the case of a linear tuned mass damper. However, the response magnitude is relatively insensitive to the exact value of the damping parameters of the mass damper, and it is therefore not important to know the magnitude of the vibration too accurately.

Finally, advantages and disadvantages of using linear or nonlinear tuned mass dampers will shortly be discussed. The conventional linear tuned mass damper has the advantage that the tuning is independent of the response magnitude and excitation intensity. However, it should be mentioned, that the optimum for the damping coefficient is very flat, see Fig. 7, so this is not a major advantage of the linear tuned mass damper over the choice of a nonlinear tuned mass dampers. Many commercially available dampers based on new materials, e.g. elastomeric dampers [9], behave in a strongly nonlinear way. Since some of these dampers have very high capacity relative to their size, it could be an economical advantage to use them rather than conventional linear viscous dampers. Finally, it should be mentioned, that it may be an advantage to have a damper with power-law viscous damping, since this limits the force for large velocities, if the power-law exponent is smaller than 1.

Acknowledgments

The present project has been supported by the Danish Technical Research Council. Part of the work was carried out, while the author was a visiting scholar at the Smart Structures Technology Laboratory, Department of Civil and Environmental Engineering, University of Illinois at Urbana-Champaign. The support is gratefully acknowledged.

Appendix A. Example of design procedure

In order to demonstrate the design procedure the case of a tuned mass damper with a viscous power-law damping is considered (Example 1). As mentioned earlier, this type of damping has been shown to give a reasonable representation of the Jarret Elastomeric Spring Damper, Terenzi [9]. The structural mass m_1, structural damping coefficient c_1 and structural stiffness k_1 are assumed to be known, along with the power-law exponent v. The spring stiffness k_2 and nonlinear damper coefficient β are the design parameters to be determined. It should be mentioned that choosing $c_1 = 0$ or very small (for lack of knowledge) gives a conservative design. The design procedure can be carried out in the following four steps:

1. Initially, the magnitude of the secondary mass m_2 must be chosen. If the necessary increase in the damping ratio $\Delta\zeta$ is known, μ can be determined from Fig. 3, and the secondary mass is then obtained from Eq. (7a).
2. The second step is to determine the optimal parameters γ^{opt} and ζ_2^{opt} for the equivalent linear system. These can be determined from Eqs. (20a,b), which is exact for $\zeta_1 = 0$, and a close approximation for $\zeta_1 \lesssim 0.3$.
3. The third step is to find the optimal damping coefficient η^{opt} for the non-dimensional nonlinear tuned mass damper. This parameter can be determined from Eq. (35), with $\sigma_{\dot{y}_2}$ given by Eq. (15), where $S_U = 2\zeta/\pi$ as seen by Eq. (8).
4. Finally, k_2 and β are determined. k_2 can be obtained in a straight forward way from Eqs. (7b) and (7c). β is evaluated from Eq. (32), which requires knowledge of $\pi S_W/c_1 = x_0^2 k_1/m_1^2$, see Eq. (4). In reality, the tuned mass damper would typically be used for wind load, which is a broad band process, but not a white noise. The most logical approach (in the authors opinion) is therefore to estimate x_0, which would then be the standard deviation of the displacement of the bare structure under critical wind conditions. S_W is then the intensity of an equivalent white noise generating a structural displacement of the same magnitude, and thereby a somewhat indirect parameter.

References

[1] J.P. Den Hartog, *Mechanical Vibrations*, McGraw-Hill, New York, 1956.
[2] J.C. Snowdon, Steady-state behavior of the dynamic absorber, *Journal of the Acoustical Society of America* 31 (1959) 1096–1103.
[3] G.B. Warburton, E.O. Ayorinde, Optimum absorber parameters for simple systems, *Earthquake Engineering and Structural Dynamics* 8 (1980) 197–217.
[4] E.O. Ayorinde, G.B. Warburton, Minimizing structural vibrations with absorbers, *Earthquake Engineering and Structural Dynamics* 8 (1980) 219–236.
[5] G.B. Warburton, Optimum absorber parameters for minimizing vibration response, *Earthquake Engineering and Structural Dynamics* 9 (1981) 251–262.
[6] G.B. Warburton, Optimum absorber parameters for various combinations of response and excitation parameters, *Earthquake Engineering and Structural Dynamics* 10 (1982) 381–401.
[7] S. Ankireddi, H.T.Y. Yang, Simple ATMD control methodology for tall buildings subject to wind loads, *Journal of Structural Engineering* 122 (1996) 83–91.
[8] F. Ricciardelli, A.D. Pizzimenti, M. Mattei, Passive and active mass damper control of the response of tall buildings to wind gustiness, *Engineering Structures* 25 (2003) 1199–1209.
[9] G. Terenzi, Dynamics of SDOF systems with nonlinear viscous damping, *Journal of Engineering Mechanics* 125 (1999) 956–963.
[10] L. Gaul, R. Nitsche, Fristion control for vibration suppression, *Mechanical Systems and Signal Processing* 14 (2000) 139–150.
[11] J.A. Inaudi, J.M. Kelly, Mass damper using friction-dissipating device, *Journal of Engineering Mechanics* 121 (1995) 142–149.
[12] F. Ricciardelli, B.J. Vickery, Tuned vibration absorbers with dry friction damping, *Earthquake Engineering and Structural Dynamics* 28 (1999) 707–724.
[13] S.R.K. Nielsen, *Linear Stochastic Vibration Theory*, Aalborg Tekniske Universitetsforlag, 1997.
[14] J.B. Roberts, P.D. Spanos, *Random Vibration and Statistical Linearization*, Wiley, Chichester, 1990.

[15] I.S. Gradshteyn, I.M. Ryzhik, *Table of Integrals, Series and Products*, fourth ed., Academic Press, London, 1965.
[16] C.C. Chang, Mass dampers and their optimal designs for building vibration control, *Engineering Structures* 21 (1999) 454–463.
[17] R.W. Clough, J. Penzien, *Dynamics of Structures*, McGraw-Hill, New York, 1975.
[18] W.H. Lin, A.K. Chopra, Earthquake response of elastic single-degree-of-freedom systems with nonlinear viscoelastic dampers, *Journal of Engineering Mechanics* 129 (2003) 597–606.
[19] F. Rüdinger, S. Krenk, Spectral density of an oscillator with power law damping excited by white noise, *Journal of Sound and Vibration* 261 (2003) 365–371.